Selective growth of highly crystalline hydroxyapatite in a micro-reaction cell of agar gel†

Katsuya Teshima,[*a] **SunHyung Lee,**[b] **Kunio Yubuta,**[c] **Shoko Mori,**[a] **Toetsu Shishido**[c] and **Shuji Oishi**[a]

High quality, idiomorphic hydroxyapatite (HAp) nanocrystals were directly, selectively and successfully grown on the hydrophobic/hydrophilic patterned surface *via* gel method. The patterned agar gel acted successfully as the micro reaction cell between raw materials. The HAp nanocrystals densely covered the hydrophilic surface, but their shape depended greatly on growth period. After 20 d growth, they were highly crystalline and well developed, and their crystal shape changed to form the one-dimensional (1-D) structure. Furthermore, idiomorphic, hexagonal cylindrical HAp nanocrystals were obtained after annealing at 600 °C for 5 h. It is expected to become considerably important in researching the direct growth/patterning of biocrystals.

1. Introduction

The control of crystallization in advanced functional inorganic materials is important for fabricating their composite nano/micro-devices.[1–4] In particular, formation of highly functional crystals on various material surfaces is much required for leading-edge nano/micro-devices.[5–11] In biocrystals, calcium phosphate has recently attracted considerable interest as the functional material due to its high bio-compatibility, thermal stability, adsorption properties and ion exchange properties, which make it very promising for a variety of application, such as in biomaterials, sensors, lasers and separating agents. Among these calcium phosphates, hydroxyapatite [$Ca_5(OH)(PO_4)_3$, HAp] is a highly biocompatible and well-known constituent of bones and teeth in the human body and has thus received much attention as a source for artificial bones, scaffolds for tissue engineering, and protein chromatography applications.[1,3,11–14] Bones and teeth consist of fine whiskers or plate-like crystals of a mineral closely related to carbonated HAp. These whiskers and crystals are mixed with organic collagen to form nano- or micro-composites. Extra pure, well-developed HAp crystals are there-fore of great interest for use in detailed medical applications and surgery. There have been many studies on the growth of HAp crystals using various techniques, including solid-state reaction, hydrothermal growth, plasma techniques, sol–gel crystallization, biomimetic processes *etc.*[15–22] In our previous study, well-developed octacalcium phosphate [OCP, $Ca_8H_2(PO_4)_6\cdot5H_2O$] of an apatite precursor were grown using the gel method.[23] The grown crystals were spherical in shape with whiskers radiating from the center region of the spherulites. Here, whisker is a needle-shaped single crystal with mostly theoretical strength due to their perfect geometry, not fiber. The fabrication of various devices with functional ceramics, such as biomaterials and semiconductors, required crystals with high quality, density, functionalization and micro-patterning on the solid substrate. Simultaneously achieving the desired density and pattern was very difficult due to the requirements of unique nucleation, size and orientation. Crystallization can be guided by molecular recognition at inter-faces. In gels, the reactive ions and reaction condition were easily controlled; thus, a gel was used as a reaction cell for inorganic crystals. In addition, self-assembled monolayers (SAMs) have been used intensively to control surface property, such as wet properties and static electricity properties on solid substrates.[4,5,9,10] Here, we report the selective growth of high quality HAp nanocrystals *via* gel method, using the system $Ca(NO_3)_2$–$(NH_4)_2HPO_4$–agar, on a hydrophilic/hydrophobic SAM template, without using a simulated body fluid.

2. Experimental

Fig. 1(a) schematically illustrates the experimental procedure. A N-type Si (100) covered with a native oxide layer (electrical resistivity of 4–6 Ω cm^{-1}) was used as the substrate. The Si substrate was cleaned in acetone, ethanol, and deionized water, in that order. After being cleaned, the substrates were exposed to vacuum ultraviolet (VUV) light with a wavelength of 172 nm using an excimer lamp (USHIO, UER20-172VB) for 15 min under atmospheric pressure and at room temperature. This procedure simultaneously removed pollutants from the substrate surface and hydroxylated the surface. First, a hydrophobic organosilane SAM was fabricated as the template layer. A hydrophobic organosilane SAM was prepared by thermal chemical vapour deposition (CVD) from heptadecafluoro-1,1,2,2-tetra-hydrodecyl-1-trimethoxysilane [FAS-17, $CF_3(CF_2)_7$ $(CH_2)_2Si(OCH_3)_3$, Azmax]. Each of the cleaned Si substrates was placed together with glass cup filled with 200 μl of FAS-17 liquid into a Teflon container. The Teflon container was sealed and placed in an oven in which the temperature was kept at 150 °C for 3 h. The hydrophobic/hydrophilic pattern was prepared by VUV

[a]Department of Environmental Science and Technology, Faculty of Engineering, Shinshu University, Nagano, 380-8553, Japan. E-mail: teshima@shinshu-u.ac.jp

[b]Faculty of Engineering, Shinshu University, Nagano, 380-8553, Japan. E-mail: leesh@shinshu-u.ac.jp

[c]Institute for Materials Research, Tohoku University, Sendai, 980-8577, Japan. E-mail: yubuta@imr.tohoku.ac.jp

† Electronic supplementary information (ESI) available: Fig. 1 EDS spectrum and mapping data of HAp nanocrystals that were grown on the hydrophilic surface for 20 days. Fig. 2 (a) Bright-field TEM micrograph. (b) SAED pattern and (c) lattice image of typical 1-D HAp nanowhiskers. See DOI: 10.1039/c0ce00079e
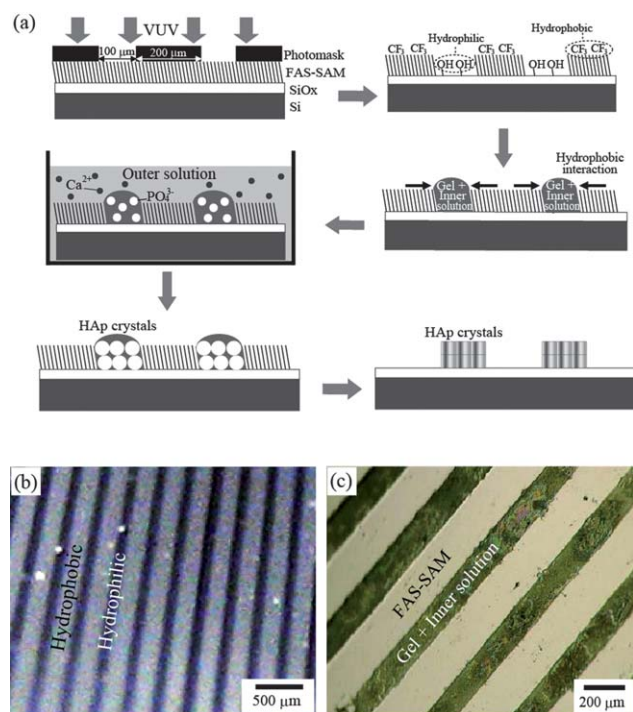
Fig. 1 (a) Schematic illustration of the experimental procedure. Optical image of (b) water and (c) the gel matrix containing 1 M $(NH_4)_2HPO_4$ aqueous solution selectively adsorbed on the photochemically patterned surface.

light irradiation conducted through a photomask under about 10 Pa pressure for 30 min. The power of the irradiated light was confined to 10 mW cm^{-2} by fixing the distance between the VUV lamp and the sample at 10 mm. The exposed FAS-SAM was removed and the exposed substrate was photochemically hydroxylated.

Next, reagent-grade $(NH_4)_2HPO_4$ and $Ca(NO_3)_2 \cdot 4H_2O$ (Wako Pure Chemical Industries) were used for growing HAp crystals. A 1 M $(NH_4)_2HPO_4$ solution (that is, inner solution) and 0.5 mass % agar was inserted in warm water at 80 °C. In addition, 1 M $Ca(NO_3)_2 \cdot 4H_2O$ was added to distilled water at room temperature and used as the outer solution. The hydrophobic/hydrophilic patterned Si substrates were dipped in the aqueous gel solution containing the inner solution to selectively adsorb on the hydrophilic surface. After being stabilized at 37 °C for 1 d, substrates were immersed in the outer solution at 37 °C for various time periods. Finally, the gel matrices were eliminated in warm water.

The obtained samples were observed using an optical microscopy, field emission scanning electron microscopy (FESEM, JEOL, JSM-7000F) operated at an accelerating voltage of 15 kV and transmission electron microscopy (TEM, JEOL, JEM-2010) operated at 200 kV. The crystal phases were studied by X-ray diffraction (XRD, Rigaku, MiniFlexII) with Cu-Kα radiation (λ = 0.154 nm). XRD measurement was obtained at 30 kV and 20 mA in the range 2θ from 3 to 60°. Fourier transform infrared spectroscopy (FTIR, JASCO, FT/IR-6100) and an energy-dispersive X-ray spectrometry (EDS, JEOL, JSM-6701F) operating at an accelerating voltage of 15 kV were used to study variation in the concentration of major constituents of the growth crystals.

3. Results and discussion

As a hydrophobic template layer, the FAS-SAM was prepared on the Si substrate by using the thermal CVD method at 150 °C for 3 h.[24] The static water contact angle of the FAS-SAM surface was about 112 ± 2°. This contact angle was considered reasonable because the static water contact angle of the CF_3 surface was 120°.[24] In addition, hydrophobic/hydrophilic templates were fabricated by VUV light irradiation conducted through a photomask. After irradiation, the substrates were dipped in water to confirm the fabrication of hydrophobic/hydrophilic pattern (Fig. 1(b)). The water molecules were selectively adsorbed on the VUV light exposed area of FAS-SAM, because the exposed FAS-SAM was photochemically decomposed and the substrate was photochemically converted to the hydroxylated surface. Thus, a hydrophobic/hydrophilic template was successfully fabricated on the Si substrate for use in the micro-scaled reaction field of HAp. Next, HAp crystals are prepared through the intermediary of agar gels from an aqueous solution of $(NH_4)_2HPO_4$ and $Ca(NO_3)_2 \cdot 4H_2O$; these are used as the inner and outer solutions, respectively. The aqueous gel solution with $(NH_4)_2HPO_4$ is selectively adsorbed on the hydrophilic surface; the resultant area is used as the micro-scaled reaction cell. Fig. 1(c) shows an optical photograph of the photochemically patterned substrate after it was dipped into the aqueous gel solution. The gel containing the inner solution of 1 M $(NH_4)_2HPO_4$ was clearly and selectively adsorbed on the hydrophilic area of the patterned substrate. In addition, the width of the adsorbed area was expanded in comparison with the width of the exposed area on photomask (width: 100 μm) because the gel was more adsorbed than the height of the FAS molecule (height: 2.2 nm).

After these samples were immersed in the outer solution for 1 to 20 d, HAp nanocrystals were selectively grown in the patterned gels. The samples were incubated in the aqueous outer solution with 1 M $Ca(NO_3)_2 \cdot 4H_2O$ at 37 °C. A bright and black linear structure was observed in the FESEM image (Fig. 2(a)) and they corresponded to the selectively grown HAp crystals and FAS-SAM, respectively. Fig. 2(b) shows highly magnified FESEM images of HAp nanocrystals grown on the hydrophilic surface for 20 d. The HAp nanocrystals densely covered the hydrophilic surface, but the shape of the grown HAp nanocrystals depended greatly on growth period. After 5 d of growth, thin plate-like structures were formed. On the other hand, HAp nanocrystals grown for 20 d were well-developed, and their crystal shape changed to form the 1-D structure shown in
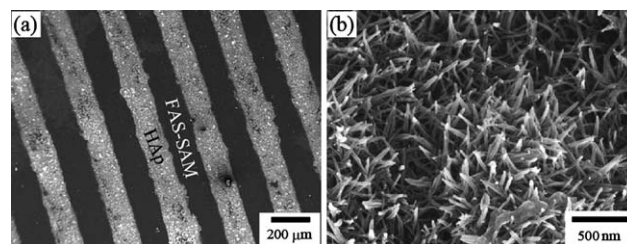

Fig. 2 (a) FESEM image of the HAp nanocrystals that were selectively grown on photochemically patterned FAS-SAM surface. (b) Highly magnified FESEM image of the HAp nanocrystals on the hydrophilic surface for 20 d.

Fig. 2(b). The surface SEM image showed that well-formed HAp nanowhiskers seem to be grown directly on the Si surface.

Fig. 3(a) shows the XRD profiles for the HAp crystals grown for 20 d. $Ca_5(OH)(PO_4)_3$ had the characteristic four diffraction peaks attributed to the (211), (112), (300) and (202) planes between 31.5 and 34.5°. The characteristic four diffraction peaks could be observed very clearly in the whiskers in Fig. 3(a). The grown nanocrystals were finally identified by their XRD pattern as $Ca_5(OH)(PO_4)_3$ using data from the literature.[25] The variations in chemical bond and the major constituents in the nanocrystals grown for 20 d were investigated by FTIR spectroscopy (Fig. 3(c) and 3(d)) and EDS (ESI 1†). In the FTIR spectra, the absorption band at approximately 3570 cm^{-1} was assigned to the stretching mode (ν_s) of the hydroxyl group, OH. The broad absorption band centered at 3400 cm^{-1} originated from adsorbed water molecules. The adsorbed water was likely formed when the crystals were separated from gel in warm water. The absorption bands at about 1090, 1025, 960, 605 and 560 cm^{-1} were assigned to vibrations of the phosphate group, PO_4^{3-}. Therefore, it was confirmed that HAp nanocrystals containing OH groups could be grown on the Si substrate. Furthermore, the $K\alpha$ lines of calcium, phosphorous and oxygen atoms were clearly detected in the EDS analysis (ESI 1†), indicating that calcium, phosphorous and oxygen atoms were distributed homogeneously in the nanocrystals, whereas potassium and nitrogen from the gel were not detected.

Fig. 4 shows the FESEM images and XRD pattern of HAp nanocrystals grown for 20 d and then annealed at 600 °C for 5 h. Idiomorphic, 1-D HAp nanocrystals were obtained after annealing. The basic form of the grown nanocrystals was
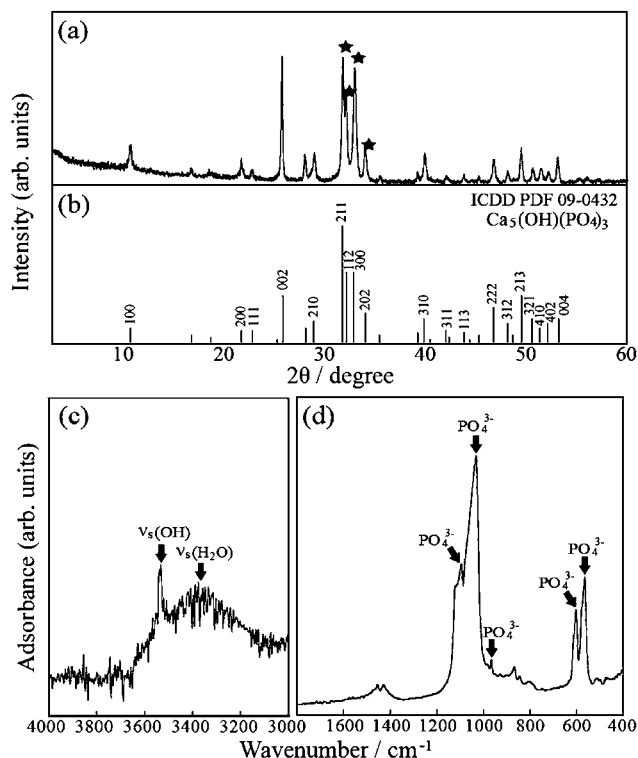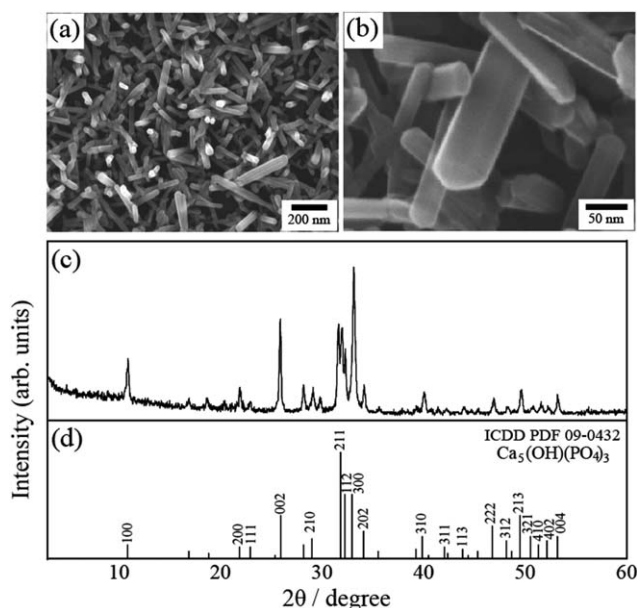

Fig. 4 (a) Lowly and (b) Highly magnified FESEM images of HAp nanocrystals annealed at 600 °C for 5 h. (c) XRD patterns of HAp nanocrystals that were grown on the hydrophilic surface for 20 d and then annealed at 600 °C for 5 h. (d) HAp ICDD PDF.[25]

a hexagonal cylinder as shown in Fig. 4(a). Hexagonal cylindrical nanocrystals with pyramidal or truncated pyramidal end faces were frequently observed (see Fig. 4(b)). Furthermore, XRD results indicated the unique 1-D nanocrystals were highly crystalline HAp (Fig. 4(c)). Hereafter, surface finishing techniques for a variety of substrates will likely become important in research on the direct growth/patterning of biocrystals.

Fig. 5 shows (a) a bright-field TEM image and (b) the corresponding selected area electron diffraction (SAED) pattern of rod-like HAp nanocrystals grown for 20 d and then annealed at 600 °C for 5 h. The bright field TEM image shown in Fig. 5(a) demonstrates that the HAp nanocrystals easily produce anisotropic growth for its columnar structure. The formation of rod-like HAp nanocrystals was confirmed from this SAED pattern (Fig. 5(b)). Fig. 5(c) shows a lattice image obtained from a 1-D (i.e., prismatic) HAp nanocrystal, wherein it can be observed that the 1-D crystal is highly crystalline because of the absence of any observable defect. ESI 2† shows (a) a bright-field TEM image and (b) the SAED pattern of typical HAp nanowhiskers grown for 20 d (without annealing). The TEM images demonstrated
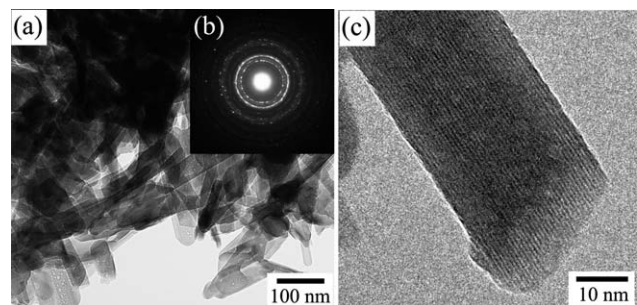

Fig. 3 XRD patterns (Cu-Kα) of (a) gel-grown crystals (growth period = 20 d) and (b) HAp ICDD PDF.[25]; (c) and (d) FTIR spectrum of HAp crystals that were selectively grown on the hydrophilic surface for 20 d.

Fig. 5 (a) Bright-field TEM micrograph, (b) SAED pattern and (c) lattice image of typical rod-like HAp nanocrystals.

that high-quality, idiomorphic HAp nanowhiskers were obviously grown for 20 d without annealing. These TEM results demonstrate that their crystallinity was hardly changed though their sizes and shapes changed greatly by annealing at 600 °C.

Crystal growth in a gel is a special case of solution growth involving controlled diffusion and convection-free growth process. The driving forces of crystal growth are ion diffusion and reaction in gel matrices. The gel growth of high-quality crystals is a self-purifying process, free from the thermal strains that are common in crystals grown from a melt. Finally, the gel technique is nature-mimetic, and is applied to the study of crystal growth in the human body, including gastric and urethral calculi. In the future, it will become more and more important to develop various functional biomaterials with the use of environmentally friendly processes.

4. Conclusion

High quality, idiomorphic HAp nanocrystals were selectively and directly grown on a hydrophilic/hydrophobic SAM template. An agar gel was successfully used as the micro reaction cell between $(NH_4)_2HPO_4$ and $Ca(NO_3)_2 \cdot 4H_2O$ solutions. FAS-SAMs were used as hydrophobic template surfaces. Hydrophilic/hydrophobic templates were photochemically fabricated by VUV light irradiation. First, the aqueous gel solution containing 1 M $(NH_4)_2HPO_4$ solution was selectively adsorbed on the hydrophilic area of the VUV light-patterned FAS-SAM surface. After immersion in an outer solution of 1 M aqueous $Ca(NO_3)_2 \cdot 4H_2O$ for 20 d, the high quality HAp nanocrystals formed the assembled whisker structure and were selectively and directly grown on the hydrophilic surface. After annealing at 600 °C for 5 h, the basic form of the grown nanocrystals was a hexagonal cylinder. Finally, our fabrication techniques of biocrystals on a variety of material surfaces are quite unique, nature-mimetic and an environmentally friendly, that is low environmental damage and low product cost.

Acknowledgements

References

1 A. H. Heuer, D. J. Fink, V. J. Laraia, J. L. Arias, P. D. Calvert, K. Kendall, G. L. Messing, J. Blackwell, P. C. Rieke, D. H. Thompson, A. P. Wheeler, A. Veis and A. I. Caplan, *Science*, 1992, **255**, 1098–1105.
2 S. Mann and G. A. Ozin, *Nature*, 1996, **382**, 313–318.
3 S. I. Stupp and P. V. Braun, *Science*, 1997, **277**, 1242–1248.
4 J. Aizenberg, A. J. Black and G. M. Whitesides, *Nature*, 1999, **398**, 495–498.
5 J. Aizenberg, A. J. Black and G. M. Whitesides, *Nature*, 1998, **394**, 868–871.
6 M. Trau, N. Yao, E. Kim, Y. Xia, G. M. Whitesides and I. A. Aksay, *Nature*, 1997, **390**, 674–676.
7 D. Palms, C. Priest, R. Sedev, J. Ralston and G. Wegner, *J. Colloid Interface Sci.*, 2006, **303**, 333–336.
8 N. Bowden, S. Brittain, A. G. Evans, J. W. Hutchinson and G. M. Whitesides, *Nature*, 1998, **393**, 146–149.
9 A. L. Briseno, J. Aizenberg, Y. J. Han, R. A. Penkala, H. Moon, A. J. Lovinger, C. Kloc and Z. Bao, *J. Am. Chem. Soc.*, 2005, **127**, 12164–12165.
10 J. F. Kang, J. Zaccaro, A. Ulman and A. Myerson, *Langmuir*, 2000, **16**, 3791–3796.
11 P. X. Zhu, Y. Masuda and K. Koumoto, *J. Colloid Interface Sci.*, 2001, **243**, 31–36.
12 E. C. Moreno, M. Kresak and R. T. Zahradnik, *Nature*, 1974, **247**, 64–65.
13 W. L. Murphy and D. J. Mooney, *J. Am. Chem. Soc.*, 2002, **124**, 1910–1917.
14 M. Wakamura, K. Hashimoto and T. Watanabe, *Langmuir*, 2003, **19**, 3428–3431.
15 J. M. Cao, J. Feng, S. G. Deng, X. Chang, J. Wang, J. S. Liu, P. Lu, H. X. Lu, M. B. Zheng, F. Zhang and J. Tao, *J. Mater. Sci.*, 2005, **40**, 6311–6313.
16 M. Cao, Y. Wang, C. Guo, Y. Qi and C. Hu, *Langmuir*, 2004, **20**, 4784–4786.
17 Y. P. Lu, S. T. Li, R. F. Zhu, M. S. Li and T. Q. Lei, *Surf. Coat. Technol.*, 2003, **165**, 65–70.
18 M. F. Hsieh, L. H. Perng and T. S. Chin, *Mater. Chem. Phys.*, 2002, **74**, 245–250.
19 T. Kawai, C. Ohtsuki, M. Kamitakahara, T. Miyazaki, M. Tanihara, Y. Sakaguchi and S. Konagaya, *Biomaterials*, 2004, **25**, 4529–4534.
20 R. Kumar, K. H. Prakash, P. Cheang and K. A. Khor, *Langmuir*, 2004, **20**, 5196–5200.
21 H. Ito, Y. Oaki and H. Imai, *Cryst. Growth Des.*, 2008, **8**, 1055–1059.
22 Q. Bao, C. Chen, D. Wang and J. Liu, *Cryst. Growth Des.*, 2008, **8**, 219–223.
23 K. Teshima, M. Sakurai, S. H. Lee, K. Yubuta, S. Ito, T. Suzuki, T. Shishido, M. Endo and S. Oishi, *Cryst. Growth Des.*, 2009, **9**, 650–652.
24 A. Hozumi, K. Ushiyama, H. Sugimura and O. Takai, *Langmuir*, 1999, **15**, 7600–7604.
25 ICDD-PDF 09–0432.